Eur. Phys. J. C (2022) 82:62
https://doi.org/10.1140/epjc/s10052-022-10010-y

THE EUROPEAN PHYSICAL JOURNAL C



Regular Article - Theoretical Physics

# Electromagnetic form factors in noncommutative space time

**A. Rafiei**[1,a], **Z. Rezaei**[2,b], **A. Mirjalili**[2,c]

[1] Physics Department, Shiraz University, Shiraz 71946-84334, Iran
[2] Physics Department, Yazd University, P.O.Box 89195-741, Yazd, Iran

Received: 15 February 2021 / Accepted: 10 January 2022


**Abstract** Electric and magnetic moment distributions are presenting by form factors (FF)s. Noncommutative space-time (NCST) includes an additional Lorentz index which are effecting on FFs. In this content we investigate electron-proton elastic scattering to impose the noncommutative effect on FFs and to obtain their physical meaning. Two Rosenbluth and polarization methods are utilized in NCST. The second method is not affected by NCST. When we resort to polarization method, the ratio of electric form factor to magnetic form factor in NCST is identical to the one in normal space time. This indicates the priority of polarization method to measure experimentally the concerned ratio as is expecting. On the other hand, the pure NC effect makes to appear an extra ratio, denoted by $R_{NC}$. If we let the variation of this quantity to cover the difference between the experimental results for Resonbluth and polarization ratio then the accepted lower limit of $\Lambda_{NC}$ as NC scale is achieved which is corresponding to 180° for the scattering angle.

## 1 Introduction

Predictions of the current models for the electromagnetic interaction of electron with the proton, provide the required motivation to perform the concerned electron-nucleon scattering experiments.

A crucial step in scattering experiments is to assume the charge on the fixed scattering center to be distributed over a limited but finite region of space. Then, one can deal with the electric form factor of nucleon which is in fact the Fourier transform of its charge distribution. The charge distribution involves one or more parameters, related to the spatial extend over which the charge is distributed, giving rise to well-defined scales in the form factor. The electric form factor may be approximated such that to yield us the root mean square radius of the charge distribution. Therefore, it is possible to parameterize the form factor by a dipole function which involves a free parameter. This parameter can be extracted by fitting the available data and then the radius of charge distribution would be determined.

In addition to electric charge form factor, for the fermion target, we would get magnetic form factor which can be casted in terms of the magnetic moment of an extensive target. In an scattering processes of a charged particle off the nucleon, the fermion current of the target, using the Gordon decomposition identity, can be expressed in terms of the magnetic moment of target that is accompanied by a form factor if the target is not a point like particle. It is obvious that at the limit of low transferred momentum, the numerical amount for both electric and magnetic moments approaches to 1 and the target seems a point like.

In this connection, it was Rosenbluth who first predicted that the magnetic moment of the proton is affected and varying outstandingly in electron scattering off the nucleon if the energy of electron beam is changing [1]. The experiments which have been done by High Energy Physics Laboratory (HEPL) at Stanford in fifth decade confirmed that the proton is not a point like particle and has an internal structure [2]. In fact, by data analysing of the electron-proton scattering, a charge radius for proton was reported to indicate that proton has a finite size [3]. An amount for proton radius has been reported recently [4,5] which is different with respect to [3] and makes a change in theoretical view to model the nucleon structure. An updated result on proton radius can be found in [6] which is based on magnetic-spectrometer-free method along with a windowless hydrogen gas target and is in agreement with the value found by two previous muonic hydrogen experiments [7,8].

On the other hand, some experiments at Jefferson Lab (JLab) have been done which were based on the double polarization method and new data for $G_{Ep}/G_{Mp}$ as the ratio for proton's electric to magnetic form factor at various

[a] e-mail: a.rafiei@shirazu.ac.ir
[b] e-mail: zahra.rezaei@yazd.ac.ir
[c] e-mail: a.mirjalili@yazd.ac.ir (corresponding author)

Published online: 23 January 2022

squared transferred momentum, $Q^2$, up to 5.6 GeV$^2$ have been reported [9,10]. Illustrating these data indicate a drastic difference with respect to the form factor results, arising out of the cross sections data where the Rosenbluth separation method is used to analyse them [11–14]. The difference between the theoretical results and also the reported experimental data of these two methods for the ratio of form factors, makes the required motivation to do a theoretical attempt to reduce this difference.

There are some methods trying to suppress the discrepancy between Resonbluth and polarization methods. The important one is the two photon exchange model [15,16]. But recent investigations indicate that this model has not been confirmed definitely from experimental point of view. More details of experimental considerations of this method can be found in [17,18]. Therefore, up to now there is not any absolute and definite method to resolve the discrepancy. Consequently, we get an opportunity to try other methods like the NCST.

In this article we consider the form factor results obtained with the cross sections data using the Rosenbluth separation method. As we referred above, comparison these results with the data from double polarization experiments, specifically at energy scale $Q^2 \geq 1\ GeV^2$ indicates a drastically difference [19]. Our idea to resolve this discrepancy is to recalculate the Rosenbluth cross section in non-commutative space time (NCST) which we follow it in this article. As a complementary task, we also recalculate the polarization method in NCST, however, the outcoming result does not indicate any different with respect to the result of normal space time. The consequence which we get is that employing NCST on Rosenbluth cross section provides some parameters which by adjusting them we may reduce the discrepancy between the results of these two methods. This is a good sign to indicate the advantage of NCST in analysing the electromagnetic form factors. One of these parameters is the noncommutative scale ($\Lambda_{NC}$) which we found it to be consistence with the reported value for this scale [20]. Many attempts have been done to determine the lower bound for this scale. We may refer to [21,22] where the NC effect is considered for Drell–Yan process. The explored scale for this case is such as $\Lambda \geq 0.4$ TeV.

We note that NCST can be considered to analysis the electric and magnetic form factors which are occurred at low energy scales. It is also applicable in many phenomena at low energy scales including DIS processes which we may refer to [21,22]. In this regard, one can resort also to [23] that is related to Lamb shift effect in hydrogen atom and in connection to muon magnetic moment, it is referred to [24]. In an argument to employ the NCST for the atomic clock, one can see [25]. There are as well some references which are justifying to utilize NCST even at lower energy scales such as the electroweak and also the Compton scattering scale [26,27]. Additionally the NCST effects have been investigated in various phenomenological aspects and consequently different bounds on noncommutative scale have been established [28–30] (for a set of references see [20,31] and references therein).

The organization of this paper is as it follows. In Sect. 2, we give a brief review on properties of NCST. Section 3 is devoted to investigate the form factors in Resonbluth and polarization methods. We deal with details in Sect. 4 how to employ the NCST effect in the two mentioned methods. Section 5 is allocated to the results and discussions. Finally, we give our conclusion in Sect. 6. Details of required and related computations are presented in the appendix.

## 2 A brief review on noncommutative space-time

The motivation to consider NCST backs to the noncommutative field theory in string theory where it has been shown that in the presence of a constant background field, the end points of an open string have noncommutative space-time properties [32,33]. It should be noted that the energy scale of NCST is not the one of the string theory. In fact, the noncommutative filed theory is considered as an effective field theory whose energy scale is the low limit of energy scale in string theory. Therefore, NCST would be applicable to analysis the issue of electric and magnetic from factors which we do it in the following sections.

Noncommutative theory leads to commutation relation between space-time coordinates as it follows [34,35]:

$$[\hat{x}^\mu\ ,\ \hat{x}^\nu] = i\theta^{\mu\nu}, \tag{1}$$

where hatted quantities are hermitian operators and $\theta^{\mu\nu}$ , is real, constant and asymmetry tensor. Equation (1) comes from the string theory through the Weyl–Moyal star product [34–36]:

$$\begin{aligned}(f\ *g)_{(x)} &= \exp\left(\frac{i}{2}\theta^{\mu\nu}\partial_\mu^y\partial_\nu^z\right) f\,(y)\,g\,(z)\,|_{y=z=x} \\ &= f\,(x)\,g\,(x) + \frac{i}{2}\,\theta^{\mu\nu}\left(\partial_\mu f\,(x)\right)\left(\partial_\nu g\,(x)\right) \\ &\quad + O\left(\theta^2\right).\end{aligned} \tag{2}$$

The Weyl–Moyal star product realization has been provided the required mathematical tools to construct the quantized gauge theories which can be used to perform the perturbative calculations in quantum chromodynamic [37].

The noncommutative relation, Eq. (1), leads to following uncertainty between the different coordinates[38]

$$\Delta x^\mu \Delta x^\nu \geq \frac{1}{2}\left|\theta^{\mu\nu}\right|. \tag{3}$$

When the gauge field theories are written in NCST, then the vertices of the standard model are modified by a Lorentz object as noncommutative tensor[39,40]. It has been shown that noncommutative field theories are not unitary for $\theta^{\mu 0} \neq 0$. Therefore, for observable measurements the proper choice is such that $\theta^{\mu 0} = 0$ [41]. Interested readers can obtain more information about NCST from the cited references of this section.

## 3 Analysing proton form factors in Rosenbluth and polarization methods

The electromagnetic form factors are crucial tools to get the sufficient knowledge about nucleon structure and to obtain precise and clear insight with respect to it. They play an important role in subatomic physics since they establish the most convenient link between experimental observation and theoretical analysis in this field. They describe internal structure of the nucleons related to electric charge and magnetization distributions. In the electron-proton elastic scattering, proton is not a point like (see Fig. 1) and its electromagnetic current is described by independent Lorentz objects, such that [42]:

$$J_{\mu}^{proton} = \bar{u}(p')[G_M(Q^2)\gamma_{\mu} + \frac{G_E(Q^2) - G_M(Q^2)}{2M(1+\tau)}(p'_{\mu} + p_{\mu})]u(p), \quad (4)$$

where $M$ and $Q^2 = -q^2$ are proton mass and squared transferred momentum by virtual photon, respectively. With $\tau = \frac{Q^2}{4M^2}$, the Sachs electric and magnetic form factors are defined as linear combinations of $F_1(Q^2)$ (Dirac form factor) and $F_2(Q^2)$ (Pauli form factor) and are given respectively by [42]:

$$G_E(Q^2) = F_1(Q^2) - \tau F_2(Q^2), \quad (5)$$

$$G_M(Q^2) = F_1(Q^2) + F_2(Q^2). \quad (6)$$

There are two methods to determine the proton form factors. In the first one that is called Rosenbluth separation method, the unpolarized electron is used to detect proton's structure. For this purpose, it is needed initially to introduce

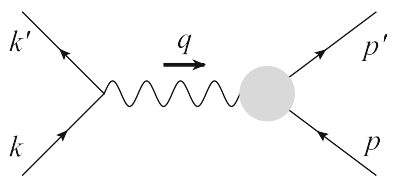


**Fig. 1** Typical schematic of Feynman diagram for electron-proton elastic scattering. Bubbled vertex indicates proton target

Mott cross section for point like particle as it follows [43,44]:

$$\left(\frac{d\sigma}{d\Omega}\right)_{Mott} = \frac{\alpha^2 \cos^2\frac{\varphi}{2}}{4E^2 \sin^4\frac{\varphi}{2}}, \quad (7)$$

where $E$ and $\varphi$ are incident energy and scattering angle, respectively. Then Rosenbluth cross section in the one-photon exchange approximation reads [1]

$$\frac{d\sigma}{d\Omega} = \left(\frac{d\sigma}{d\Omega}\right)_{Mott} \frac{1}{(1+\tau)}[G_E^2 + \frac{\tau}{\varepsilon}G_M^2], \quad (8)$$

where $\varepsilon = \left(1 + 2(1+\tau)\tan^2\frac{\varphi}{2}\right)^{-1}$ is representing polarization of the virtual photon. Consequently, the reduced cross section can be defined by:

$$\sigma_{red} = \frac{d\sigma}{d\Omega}\frac{\varepsilon(1+\tau)}{\left(\frac{d\sigma}{d\Omega}\right)_{Mott}} = \varepsilon G_E^2 + \tau G_M^2. \quad (9)$$

The $G_E^2$ as slope and $\tau G_M^2$ as intercept in Eq. (9) would be determined by fitting the measured cross section at various scattering angle $\varphi$ with fixed value for $Q^2$. In continuation, experimental data for $R = \frac{G_E}{G_M}$ [45] can be reproduced by a polynomial fit as it follows [16]:

$$\mu_p R^{\exp}_{Rosenbluth} = 1 - 0.0762\, Q^2 + 0.004896\, Q^4 + 0.001298\, Q^6, \quad (10)$$

where $\mu_p$ is the proton magnetic moment. Some experimental data for $R^{\exp}_{Rosenbluth}$ can be found in Refs. [13],[14] and [46].

As a second method to determine the proton form factors, we can resort to the polarization technique. Based on new experimental set up, the recoiled polarization technique has been employed to obtain more reliable measurements for $G_E$ and $G_M$. When the scattering electron is longitudinally polarized, i.e., its polarization vector is parallel to the momentum of the nucleon, the polarization vector of recoiled proton would be in the scattering plane. The transverse and longitudinal polarization of recoiled proton are given by [47]

$$I_0 P_T = -2\sqrt{\tau(1+\tau)}G_E G_M \tan\frac{\varphi}{2}, \quad (11)$$

$$I_0 P_L = \frac{E+E'}{M}\sqrt{\tau(1+\tau)}G_M^2 \tan^2\frac{\varphi}{2}, \quad (12)$$

where $I_0 = G_E^2 + \frac{\tau}{\varepsilon}G_M^2$. Performing the ratio of polarizations, one obtains

$$\frac{G_E}{G_M} = -\frac{P_T}{P_L}\frac{E+E'}{2M}\tan\frac{\varphi}{2}. \quad (13)$$

Experimental data for this ratio [48,49] can be reproduced by the following polynomial fit [16]:

$$\mu_p R^{\exp}_{Polarization} = 1 - 0.1306\, Q^2 + 0.004174\, Q^4 + 0.000752\, Q^6. \quad (14)$$

Numerical investigation of Eqs. (10) and (14) reveals considerable discrepancy between them which becomes more by increasing the $Q^2$ values (see Fig. 2). In the following section we are using the noncommutative effect to find a way to resolve this discrepancy.

## 4 Noncommutative proton form factor

As we referred in Sect. 2 , NCST builds an extra Lorentz object, $\theta^{\mu\nu}$, and it can be added to proton current through its vertex which yield us modified form factors. The insertion of this tensor to the leptonic vertex makes also correction on the ordinary form factors of proton but it would be absorbed effectively into the modified form factors. So the final result is such as to consider just the NCST correction on hadronic current.

Here we present the results for FFs in NCST based on the two mentioned methods.

### 4.1 Rosenbluth separation method

In this method, Eq. (4) would be modified as it follows (see the Appendix):

$$J^{proton}_{\mu} = \bar{u}(p')\Big[\tilde{G}_M\gamma_\mu + \frac{\tilde{G}_E - \tilde{G}_M}{2M(1+\tau)}(p'_\mu + p_\mu) + 2MG_{NC}\, q^\alpha \theta_{\mu\alpha}\Big]u(p), \quad (15)$$

where $G_{NC}$, $\tilde{G}_E$ and $\tilde{G}_M$ are noncommutative, electric and magnetic form factors in NCST, respectively. The last two form factors, in addition to $q^2$, depends on the other independent scalars which are made from $\theta$ tensor such as $q.\theta.p$. As noncommutative portion tends to zero, we recover normal form factors as they follow:

$$\tilde{G}_E(Q^2,\theta) \to G_E(Q^2), \quad \tilde{G}_M(Q^2,\theta) \to G_M(Q^2). \quad (16)$$

The process to obtain the scattering cross section is lengthy but it is straightly calculable. Details of calculations is inclosed in the Appendix. Considering Eq. (47) of Appendix, one can define reduced cross section as it follows

$$\sigma_{red} = \varepsilon\tilde{G}_E^2 + \tau\tilde{G}_M^2 + 2M^4G_{NC}^2|\boldsymbol{\theta}|^2\tau(1+\tau)(3+2\tau-\varepsilon). \quad (17)$$

By defining $\tilde{R} = \frac{\tilde{G}_E}{\tilde{G}_M}$ and $R_{NC} = \frac{G_{NC}}{\tilde{G}_M}$, Eq. (17) can be written as it follows:

$$\sigma_{red} = \tilde{G}_M^2 \times \left[\tau + \varepsilon\left(\tilde{R}^2 + 2R_{NC}^2M^4|\boldsymbol{\theta}|^2\tau(1+\tau)\left(\frac{3+2\tau-\varepsilon}{\varepsilon}\right)\right)\right]. \quad (18)$$

Comparing Eq. (18) with Eq. (9) and considering the definition $R = \frac{G_E}{G_M}$, one will arrive at

$$R^2_{Rosenbluth} = \tilde{R}^2 + 2R_{NC}^2M^4|\boldsymbol{\theta}|^2\tau(1+\tau)\left(\frac{3+2\tau-\varepsilon}{\varepsilon}\right). \quad (19)$$

### 4.2 Polarization method

Now we consider the proton form factor ratio in NCST but based on the polarization method. In this regard, we investigate separately each component of proton current in NCST. The timelike component of the Eq. (15) can be written as:

$$J^0 = \bar{u}(p')\Big[\tilde{G}_M\gamma^0 + \frac{\tilde{G}_E - \tilde{G}_M}{2M(1+\tau)}(p+p')^0 + 2MG_{NC}\, q_\alpha\theta^{0\alpha}\Big]u(p). \quad (20)$$

In this case, the noncommutative term would be vanished due to the property that $\theta^{0\alpha} = 0$ [41]. Hence, we have formal result for timelike component. The calculations of spacelike component in NCST is straightforward (for details see the Appendix). By substituting Eq. (61) into Eq. (60) of Appendix, proton's form factor ratio in NCST is obtained and we would get:

$$-\frac{E+E'}{2M}\frac{P_T}{P_L}\tan\frac{\varphi}{2} = \frac{\tilde{G}_E}{\tilde{G}_M}. \quad (21)$$

Comparing Eq. (21) with Eq. (13) will lead to the following result:

$$R_{polarization} = \tilde{R}. \quad (22)$$

## 5 Results and discussions

Noncommutative proton form factor has been evaluated, considering the Rosenbluth and polarization methods. We suppose that the ratio of form factor in NCST ($\tilde{R}$) is given by identical expression in these two methods. Therefore by combining Eq. (19) with Eq. (22) we find that:

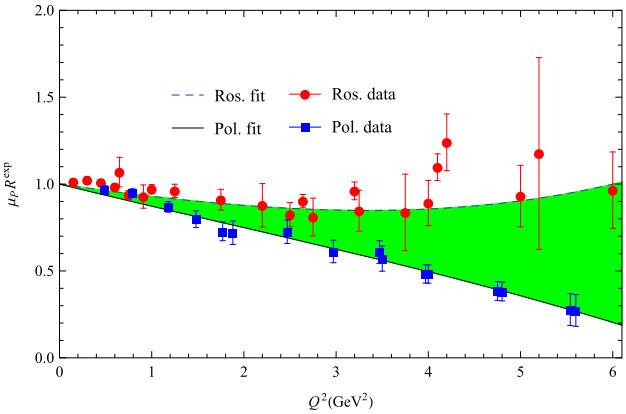


**Fig. 2** The ratio of electric and magnetic form factor in Rosenbluth and polarization methods. By slight changing the scattering angle around $\varphi \sim 180°$ the $\mu_p R_{NC}$ would reproduce the green region. The experimental data in Rosenbluth and polarization methods are quoted respectively from [13,14,45,46] and [9,10,48–51]

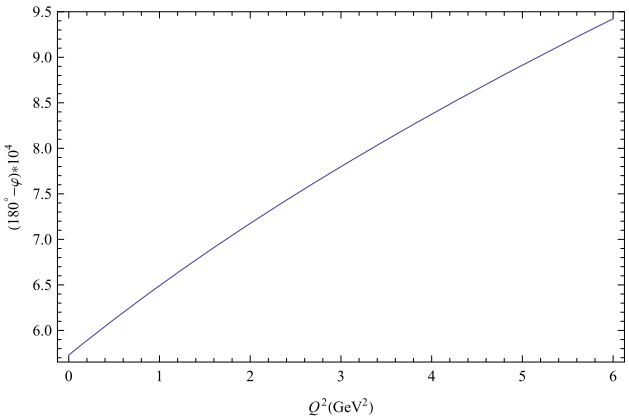


**Fig. 3** Scattering angle verses transferred momentum ($Q^2$) in NCST, taking $\Lambda_{NC} = 1$ TeV and $\varepsilon = 10^{-11}$, occurred at $\varphi \sim 180°$. As can be seen the scattered angle does not depend strongly on $Q^2$

$$\mu_p R_{NC} = \frac{\Lambda_{NC}^2}{M^2}\sqrt{\frac{1}{2\tau(1+\tau)}\left(\frac{\varepsilon}{3+2\tau-\varepsilon}\right)\left[\mu_p^2 R^2_{Rosenbluth} - \mu_p^2 R^2_{polarization}\right]} \tag{23}$$

The left hand side of Eq. (23) is again a ratio of form factors but is purely arisen from NC effect (see the Appendix). One can find that this quantity depended on $\Lambda_{NC}$ as noncommutative scale. Lower limit of this scale, reported from scattering experiments is about 1 TeV [20]. We plot Fig. 2 such as the blank region between the solid and dashed curves of polarization and Rosenbluth methods is filled by varying $\mu_p R_{NC}$. For this purpose, we fix $\Lambda_{NC}$ at 1 TeV, corresponding to the acceptable reported value [20,21,31] and eventually take $\varepsilon \sim 10^{-11}$ that is related to $\varphi \sim 180°$ as scattering angle. By slight changing this angle around $\sim 180°$, the blank region in Fig. 2 is covered which is indicated by green color. Choosing $\varepsilon \sim 10^{-11}$ and in continuation $\varphi \sim 180°$ leads to important result. To detect the effect of NCST, we need to search and examine the backward scattering region($\varphi \sim 180°$). It is a reason for hard detecting the effect of NCST in performed experiments. In other words, in order to detect the NCST effect experimentally we should look for this effect in scattering angle around 180° which is hard to adjust the experimental set up in the backward angle but eventually it is possible to do it.

Now we can say briefly that the $R_{NC}$ can approach to both the experimental data for polarization and Rosenblouth methods if we take $\Lambda_{NC}$ meets its acceptable lower limit and to let the scattering angle to vary about 180° with respect to incident beam in scattering experiments. The variation of $\varepsilon$ versus the transferred momentum is too small as can be seen in Fig. 3. Nonetheless, as we told before, we can change it slightly in order the $\mu_p R_{NC}$ to cover the blank region between Rosenbluth and polarization data . Due to small variation of $\varepsilon$ with respect to $Q^2$, the scattering angle does not also depend strongly on the transferred momentum of exchanged photon. If one is looking for NCST effect, as we refereed above, it would be occurred in the backward region. Therefore, this region should be investigated seriously and with precise attention. We should mention that the small variations of backward scattering angle with respect to $Q^2$ values does not mean that the NCST effect is tiny. It just indicates, as we said before, that the backward angle where the NCST effect should be observed there, does not depend dominantly on transferred momentum.

In connection to the NC effect, the following inference would also be catched. We assume that particles have the NC form factor and now we can also suppose that particles also contain spherical NC covering with radius $r_{NC}$. Then Eq. (3) induces a minimal area, i.e., $2s \simeq |\theta^{\mu\nu}| = \frac{1}{\Lambda^2}$ [20]. Considering the spherical surface relation ($s = 4\pi r_{NC}^2$) and substituting NC scale there, we would get

$$\Lambda_{NC} = \frac{0.28}{r_{NC}}. \tag{24}$$

Since we do not have yet evidence for NCST up to quark's size, therefore lower size for NCST would be such as $r_{NC} \leq 10^{-19}$ m, corresponding to the predicted size for quarks. Substituting this numerical bound in Eq. (24) we achieve $\Lambda \geq 400\,\text{GeV}$ that is in agreement with other NC scale bounds, obtained through scattering process [20].

## 6 Conclusion

One of the essential ingredient which can be used to reveal us the internal structure of nucleon is the electric and magnetic form factors. Since the first scattering experiments of electron beam off the nucleon in fifth decade of the twenty century, many data have been collected which confirm that the nucleon is not point like charge. By analysing the data, one can attribute to nucleon a charge distribution and following that magnetic moment of nucleon would get an anomaly value.

In this regard, primarily attempts have been done by Rosenbluth which provide us analytical result for the ratio of electric to magnetic form factors, $R = \frac{G_E}{G_M}$. Following that, the concerned data can be extracted for this ratio from proportional experiment. After then, new theoretical method is demonstrated to determine the proton form factors which is based on the polarization technique in which the longitudinal and transverse polarizations of electron beam are taken into account.

Theoretical results and experimental data for the concerned ratio are drastically different in these two methods which demand to find a way to control this discrepancy or to reduce it. One of the solution way is to consider the form factors in NCST. This is what we did in this article. The result for $R$ ratio in polarization method is not affected in NCST but the Rosenbluth one would be changed. This indicates the priority of polarization method with respect to the other method to investigate the proton form factor. Comparison the results of the two methods in NCST will yield us a quantity which is particular to NCST and is denoted in this article by $R_{NC}$ which involves some quantities like noncommutative scale $\Lambda_{NC}$ and scattering angle $\varphi$. By keeping the $\Lambda_{NC}$ scale to the accepted and reported value from DIS experiment, one is needed to take the scattering angle around 180°. By slight changing this angle and plotting the result for $R_{NC}$, we can cover the blank region between the plots of Rosenbluth and polarization methods which is depicted by green color in Fig. 2. Therefore, $\Lambda_{NC}$ resulted from noncommutative computations, is a quantity which can control the discrepancy between the results of two mention methods and in fact provide us a way to move from a region around polarization method to Rosenbluth one and makes a link between these two methods in order to adapt them with each other .

Illustrating the discrepancy of the two mentioned method can also be done by considering other effect like Lorantz violation which we hope to report on this issue in future.

**Acknowledgements** A. R. is thankful Shiraz university and the rest of authors are grateful Yazd university to provide the required facilities to do this project.

**Data Availability Statement** This manuscript has no associated data or the data will not be deposited. [Authors' comment: The required data can be found in the text and references of this article.]


Funded by SCOAP[3].

## Appendix

**Rosenbluth formula in NCST**:

Cross section for elastic electron-proton scattering in the laboratory frame is given by [43,52]

$$\frac{d\sigma}{d\Omega} = \frac{\overline{|\mathcal{M}|^2}}{64\pi^2 M^2}\left(\frac{E'}{E}\right)^2, \tag{25}$$

where $E$ and $E'$ are the energy of incident and scattered electrons (see Fig. 1).The invariant amplitude is obtained, contracting leptonic tensor with hadronic one:

$$\overline{|\mathcal{M}|^2} = \frac{e^4}{q^4} L^{\mu\nu} W_{\mu\nu}. \tag{26}$$

Leptonic tensor is already calculated and given by [20,43,52]

$$L^{\mu\nu} = 2\{k^\mu k'^\nu + k^\nu k'^\mu - g^{\mu\nu}(k.k' - m^2)\}. \tag{27}$$

For hadronic tensor one can write $W_{\mu\nu} = J_\mu J_\nu^\dagger$ where transition current for proton is given by [43]:

$$J_\mu^{proton} = \bar{u}(p')\Gamma_\mu u(p). \tag{28}$$

Here $\Gamma_\mu$ is Lorentz vector and performs the required Lorentz object. In NCST the proton vertex factor involves extra Lorentz objects with respect to normal space-time such that [53]:

$$\begin{aligned}\Gamma_\mu = {} & A\,\gamma_\mu + B\,p'_\mu + C\,p_\mu + i\,D\,p'^\nu\sigma_{\mu\nu} + i\,E\,p^\nu\sigma_{\mu\nu} \\ & + F\,p'^\nu\theta_{\mu\nu} + G\,p^\nu\theta_{\mu\nu}.\end{aligned} \tag{29}$$

In the above equation the last two terms are due to NCST. Now if we employ current conservation equation, $q_\mu J^\mu = 0$ and considering the improved transition current, we find

that $B = C$, $D = -E$, $F = -G$. Taking also Gordon decomposition relation [43], we will get:

$$J_{\mu}^{proton} = \bar{u}(p')\Big[(\tilde{F}_1 + \tilde{F}_2)\,\gamma_\mu - \frac{\tilde{F}_2}{2M}(p'_\mu + p_\mu) + 2M F_4\, q^\alpha \theta_{\mu\alpha}\Big]u(p). \tag{30}$$

Using the definition of Sachs form factors, given by Eqs. (5) and (6) and considering $G_{NC} = F_4$ then Eq. (30) can be rewritten as it follows:

$$J_{\mu}^{proton} = \bar{u}(p')\Big[\tilde{G}_M\gamma_\mu + \frac{\tilde{G}_E - \tilde{G}_M}{2M(1+\tau)}(p'_\mu + p_\mu) + 2M G_{NC}\, q^\alpha \theta_{\mu\alpha}\Big]u(p). \tag{31}$$

We should multiply Eq. (31) with its complex conjugate to obtain the hadronic tensor. Then averaging and summing over initial and final spins and considering Casimir's trick [20] will lead us to:

$$\begin{aligned} W_{\mu\nu} = {} & \frac{1}{2}Tr\Big[(\not{p} + M)\Big\{\tilde{G}_M\,\gamma_\mu + \frac{\tilde{G}_E - \tilde{G}_M}{2M(1+\tau)}(p'_\mu + p_\mu)\Big\} \\ & \times(\not{p}' + M)\Big\{\tilde{G}_M\,\gamma_\nu + \frac{\tilde{G}_E - \tilde{G}_M}{2M(1+\tau)}(p'_\nu + p_\nu)\Big\}\Big] \\ & + \frac{1}{2}Tr\Big[(\not{p} + M)\Big\{\tilde{G}_M\,\gamma_\mu + \frac{\tilde{G}_E - \tilde{G}_M}{2M(1+\tau)}(p'_\mu + p_\mu)\Big\} \\ & \times(\not{p}' + M)\{2M G_{NC}\, q^\beta \theta_{\nu\beta}\}\Big] + \frac{1}{2}Tr \\ & \times\Big[(\not{p} + M)\{2M G_{NC}\, q^\alpha \theta_{\mu\alpha}\}(\not{p}' + M) \\ & \times\Big\{\tilde{G}_M\,\gamma_\nu + \frac{\tilde{G}_E - \tilde{G}_M}{2M(1+\tau)}(p'_\nu + p_\nu)\Big\}\Big] \\ & + \frac{1}{2}Tr[(\not{p} + M)\{2M G_{NC}\, q^\alpha \theta_{\mu\alpha}\} \\ & \times(\not{p}' + M)\{2M G_{NC}\, q^\beta \theta_{\nu\beta}\}]. \end{aligned} \tag{32}$$

This equation have three contributions with respect to non-commutative tensor, $\theta_{\mu\nu}$. The first term is zeroth order of $\theta$ that is in fact the normal form of hadronic tensor. By contracting leptonic tensor, given by Eq. (27), with first contribution of the hadronic tensor in above, we will get the mean square invariant amplitude like the one in normal case [43]

$$\overline{|\mathcal{M}_0|^2} = \frac{e^4}{q^2}4M^2Q^2\left[\frac{\tilde{G}_E^2 + \tau\tilde{G}_M^2}{1+\tau}\cot^2\frac{\varphi}{2} + 2\tau\tilde{G}_M^2\right]. \tag{33}$$

As can be seen the second and third term in Eq. (32) are linear with respect to $\theta$. Using trace theorems and doing straightforward calculations we reach to below result from the $\theta$ linear contribution of hadronic tensor in Eq. (32):

$$W^1_{\mu\nu}(\theta) = +4M^2 G_{NC}\tilde{G}_E\,[(\theta.q)_\nu(p_\mu + p'_\mu) + (\theta.q)_\mu(p_\nu + p'_\nu)], \tag{34}$$

where $(\theta.q)_\mu = \theta_{\mu\alpha}q^\alpha$. Also, we could simplify it more by taking into account the scalar product $p.p' = M^2(1 - \frac{q^2}{2M^2})$ in the laboratory frame. Now by contracting it with leptonic tensor, Eq. (27), we find that

$$\begin{aligned} \overline{|\mathcal{M}_1(\theta)|^2} = {} & \frac{e^4}{q^4}16M^2G_{NC}\tilde{G}_E\{+(k'.\theta.q)(k.p + k.p') \\ & +(k.\theta.q)(k'.p + k'.p') \\ & -(k.k')(p.\theta.q + p'.\theta.q)\}, \end{aligned} \tag{35}$$

where we neglected the electron's mass, $m$. By replacing $q = k - k' = p' - p$ (see Fig. 1) into above equation, using Eq. (1) and considering the momentum of initial proton in the laboratory frame, $p \equiv (M, \mathbf{0})$, we arrive at:

$$\overline{|\mathcal{M}_1(\theta)|^2} = \frac{e^4}{q^4}32M^2G_{NC}\tilde{G}_E(k'.\theta.k)(k.p + k'.p). \tag{36}$$

Finally, we carry out the fourth term in Eq. (32) that is of second order with respect to $\theta^2$. The similar calculations can be repeated for this part of hadronic tensor which lead us to

$$\begin{aligned} W^2_{\mu\nu}(\theta^2) &= 2M^2G^2_{NC}\left(Tr[\not{p}\,\not{p}'] + M^2Tr[1]\right)q^\alpha\theta_{\mu\alpha}q^\beta\theta_{\nu\beta} \\ &= 2M^2G^2_{NC}\left(4(p.p') + 4M^2\right)q^\alpha\theta_{\mu\alpha}q^\beta\theta_{\nu\beta} \\ &= 8M^4G^2_{NC}\left(\frac{p.p'}{M^2} + 1\right)q^\alpha\theta_{\mu\alpha}q^\beta\theta_{\nu\beta}. \end{aligned} \tag{37}$$

Using again $p.p' = M^2(1 - \frac{q^2}{2M^2})$ we will get

$$W^2_{\mu\nu}(\theta^2) = 16M^4G^2_{NC}\,(1+\tau)\,q^\alpha\theta_{\mu\alpha}q^\beta\theta_{\nu\beta}. \tag{38}$$

By contracting Eq. (38) to the leptonic tensor, Eq. (27), the mean square invariant amplitude would be obtained as it follows

$$\begin{aligned} \overline{|\mathcal{M}_2(\theta^2)|^2} = {} & \frac{e^4}{q^4}32M^4G^2_{NC}\,(1+\tau)\{2(k.\theta.q)(k'.\theta.q) \\ & +(k.k')(q.\theta.\theta.q)\}. \end{aligned} \tag{39}$$

Now to simplify the above equation, by taking $\alpha$, $\beta$ and $\gamma$ as angles between $\mathbf{k}$, $\mathbf{k}'$, $\mathbf{k}\times\mathbf{k}'$ and $\boldsymbol{\theta}$ direction, respectively, in the laboratory frame we will get [20]:

$$k.\theta.\theta.k = E^2|\boldsymbol{\theta}|^2\sin^2\alpha, \tag{40}$$

$$k'.\theta.\theta.k' = E'^2|\boldsymbol{\theta}|^2\sin^2\beta, \tag{41}$$

$$k.\theta.\theta.k' = E\,E'|\boldsymbol{\theta}|^2(\cos\varphi - \cos\beta\cos\alpha), \tag{42}$$

$$k.\theta.k' = E\,E'|\boldsymbol{\theta}|\sin\varphi\cos\gamma. \tag{43}$$

Then by taking the average over $\alpha$, $\beta$ and $\gamma$, Eq. (36) will be vanished and does not have contribution to total mean square invariant amplitude, therefore Eq. (39) is simplified to:

$$\overline{|\mathcal{M}_2(\theta^2)|^2} = \frac{e^4}{q^4} 16M^4 G_{NC}^2 (1+\tau) Q^2 |\boldsymbol{\theta}|^2 \times \left[ EE' + \frac{Q^2}{2}(1+\tau) \right]. \tag{44}$$

Summing Eqs. (33) and (44), the total mean squared invariant would be gained as in below:

$$\begin{aligned}\overline{|\mathcal{M}_{tot}|^2} &= \overline{|\mathcal{M}_0|^2} + \overline{|\mathcal{M}_2(\theta^2)|^2} \\ &= \frac{e^4}{q^2} 4M^2 Q^2 \left[ \frac{\tilde{G}_E^2 + \tau \tilde{G}_M^2}{1+\tau} \cot^2\frac{\varphi}{2} + 2\tau \tilde{G}_M^2 \right. \\ &\quad \left. + 4M^2 G_{NC}^2 (1+\tau) |\boldsymbol{\theta}|^2 (EE' + \frac{Q^2}{2}(1+\tau)) \right].\end{aligned} \tag{45}$$

Then replacing Eq. (45) into Eq. (25) and doing some manipulations we find that:

$$\begin{aligned}\frac{d\sigma}{d\Omega} &= \frac{\alpha^2}{4E^2 \sin^4\frac{\varphi}{2}} \frac{E'}{E} \cos^2\frac{\varphi}{2} \\ &\times \left[ \frac{\tilde{G}_E^2 + \tau \tilde{G}_M^2}{1+\tau} + 2\tau \tilde{G}_M^2 \tan^2\frac{\varphi}{2} + 4M^2 G_{NC}^2 (1+\tau) |\boldsymbol{\theta}|^2 \right. \\ &\times \left. \left( EE' + \frac{Q^2}{2}(1+\tau) \right) \tan^2\frac{\varphi}{2} \right].\end{aligned} \tag{46}$$

By defining $\varepsilon = \left(1 + 2(1+\tau)\tan^2\frac{\varphi}{2}\right)^{-1}$ and using Eq. (7) the final result would be:

$$\begin{aligned}\frac{d\sigma}{d\Omega} &= \left(\frac{d\sigma}{d\Omega}\right)_{Mott} \frac{1}{(1+\tau)\varepsilon} \left[ \varepsilon \tilde{G}_E^2 + \tau \tilde{G}_M^2 \right. \\ &\quad \left. + 2M^4 G_{NC}^2 |\boldsymbol{\theta}|^2 \tau (1+\tau)(3 + 2\tau - \varepsilon) \right]\end{aligned} \tag{47}$$

**Polarization method in NCST**

Starting point is Eq. (31) that has been written in NCST. In the following we are going to investigate the timelike and spacelike components of $\theta^{\mu\nu}$ separately. First we consider timelike component and using $\theta^{0\alpha} = 0$. Consequently the proton's current is converted to the normal one. Thus, using Dirac spinors for initial and final proton states, one can write

$$u(p) = \sqrt{E+M} \begin{pmatrix} \chi \\ \frac{\boldsymbol{\sigma}.\mathbf{p}}{E+M}\chi \end{pmatrix}, \tag{48}$$

$$u^\dagger(p') = \sqrt{E'+M} \begin{pmatrix} \chi^{\dagger\prime} & \frac{\boldsymbol{\sigma}.\mathbf{p}'}{E'+M}\chi^{\dagger\prime} \end{pmatrix}, \tag{49}$$

where the methodology of Ref. [52] has been used. Here $\boldsymbol{\sigma}$ is representing the Pauli matrices which are satisfying the identity $(\boldsymbol{\sigma}.\mathbf{p})^2 = p^2$.

Considering the incoming and outgoing momentum of proton in the Breit frame which have just the $z$ component such that $p^\mu = \left(M\sqrt{1+\tau}, 0, 0, -\frac{Q}{2}\right)$ and $p'^\mu = \left(M\sqrt{1+\tau}, 0, 0, \frac{Q}{2}\right)$, we will arrive at:

$$\begin{aligned}J^0 &= (E+M) \left[ \tilde{G}_M \left( 1 - \frac{\mathbf{p}^2}{(E+M)^2} \right) \right. \\ &\quad \left. + \frac{\tilde{G}_E - \tilde{G}_M}{\sqrt{1+\tau}} \left( 1 + \frac{\mathbf{p}^2}{(E+M)^2} \right) \right] \chi^{\dagger\prime}\chi,\end{aligned} \tag{50}$$

In the Breit frame one can deduce $\mathbf{p}' = -\mathbf{p}$ and $E = E' = M\sqrt{1+\tau}$ which help us to simplify Eq. (50) as it follows:

$$J^0 = 2M\tilde{G}_E \chi^{\dagger\prime}\chi. \tag{51}$$

For spacelike component one can write

$$\mathbf{J}^k = \bar{u}(p')[\tilde{G}_M \gamma^k + 2MG_{NC}\, q_\alpha \theta^{k\alpha}]u(p). \tag{52}$$

On the other hand using $\theta_{ij} = \frac{1}{2}\varepsilon_{ijk}\theta_k$, the following identity would be obtained

$$\begin{aligned}q_\alpha \theta^{k\alpha} &= -q_i \theta^{ki} = -q_i \left( \frac{1}{2}\varepsilon_{ikj}\theta_j \right) = -\frac{1}{2}\varepsilon_{jik}\theta_j q_i \\ &= -\frac{1}{2}\boldsymbol{\theta} \times \mathbf{q} = \frac{1}{2}\mathbf{q} \times \boldsymbol{\theta}.\end{aligned} \tag{53}$$

After some manipulations, Eq. (52) is simplified as it follows:

$$\mathbf{J} = 2i\tilde{G}_M \chi^{\dagger\prime} \mathbf{p} \times \sigma\chi + 2M^2 G_{NC}\, \mathbf{q} \times \boldsymbol{\theta}\sqrt{1+\tau}\chi^{\dagger\prime}\chi. \tag{54}$$

Presenting the components of $\boldsymbol{\theta}$ as $\boldsymbol{\theta} = |\theta|(\sin\eta\ \cos\lambda, \sin\eta\ \sin\lambda, \cos\eta)$ and considering the four vector $q$ in Berit frame such that $q^\mu = (0, 0, 0, Q)$ then we can write

$$\mathbf{p} \times \boldsymbol{\sigma} = (0, 0, -\frac{Q}{2}) \times (\sigma_x, \sigma_y, \sigma_z) = \frac{Q}{2}\sigma_y \hat{x} - \frac{Q}{2}\sigma_x \hat{y}, \tag{55}$$

$$\mathbf{q} \times \boldsymbol{\theta} = (0, 0, Q) \times (\theta_1, \theta_2, \theta_3) = -Q\theta_2 \hat{x} + Q\theta_1 \hat{y}. \tag{56}$$

Then $J^\mu$ in the matrix form would be appeared as:

$$J^\mu = \begin{pmatrix} 2M\tilde{G}_E \chi'^\dagger \chi \\ +iQ\tilde{G}_M \chi'^\dagger \sigma_y \chi \ -2M^2 Q\theta_2 G_{NC}\sqrt{1+\tau}\ \chi'^\dagger\chi \\ -iQ\tilde{G}_M \chi'^\dagger \sigma_x \chi + 2M^2 Q\theta_1 G_{NC}\sqrt{1+\tau}\ \chi'^\dagger\chi \\ 0 \end{pmatrix}. \tag{57}$$

Multiplying $J^\mu$, Eq. (57), with its complex conjugate and using completeness relation $\sum_s \chi\chi^\dagger = 1$ and averaging over

initial spin state, $\eta$ and $\lambda$, we can write the hadronic tensor as $W^{\mu\nu} = W_A^{\mu\nu} + W_S^{\mu\nu}$ where:

$$W_A^{\mu\nu} = \frac{1}{2}\begin{pmatrix} 0 & -2iMQ\tilde{G}_E\tilde{G}_M\chi'^{\dagger}\sigma_y\chi' & 2iMQ\tilde{G}_E\tilde{G}_M\chi'^{\dagger}\sigma_x\chi' & 0 \\ 2iMQ\tilde{G}_E\tilde{G}_M\chi'^{\dagger}\sigma_y\chi' & 0 & iQ^2\tilde{G}_M^2\chi'^{\dagger}\sigma_z\chi' & 0 \\ -2iMQ\tilde{G}_E\tilde{G}_M\chi'^{\dagger}\sigma_x\chi' & -iQ^2\tilde{G}_M^2\chi'^{\dagger}\sigma_z\chi' & 0 & 0 \\ 0 & 0 & 0 & 0 \end{pmatrix}, \tag{58}$$

and following that

$$W_S^{\mu\nu} = \frac{1}{2}\begin{pmatrix} 4M^2\tilde{G}_E^2 & 0 & 0 & 0 \\ 0 & Q^2\tilde{G}_M^2 + L^2Q^2G_{NC}^2 & 0 & 0 \\ 0 & 0 & Q^2\tilde{G}_M^2 + L^2Q^2G_{NC}^2 & 0 \\ 0 & 0 & 0 & 0 \end{pmatrix}, \tag{59}$$

where $L^2 = M^4|\theta|^2(1+\tau)$. Explicitly, Eq. (58) shows that noncommutative contributions drop out from calculations, while for finding transverse and longitudinal polarization ($P_T$, $P_L$) ratio we need to investigate $L^A_{\mu\nu}W_A^{\mu\nu}$ in $\hat{x}$ and $\hat{z}$-direction, respectively. Therefore, by contraction $L^A_{\mu\nu}$ (that obtained in Ref. [52]) with Eq. (58) and evaluate it in the $\hat{x}$ and $\hat{z}$-direction and takeing the trace from arisen result, we will arrive at

$$\frac{P_T}{P_L} = \frac{L^A_{\mu\nu}W_A^{\mu\nu}(\hat{x})}{L^A_{\mu\nu}W_A^{\mu\nu}(\hat{z})} = -\frac{\tilde{G}_E}{\tilde{G}_M}\frac{2M}{Q}\cos\frac{\varphi_B}{2}, \tag{60}$$

where $\varphi_B$ is the scattering angle in the Breit frame. Finally if we utilize the relation between scattering angle in the Breit and laboratory frame, we will get for $\varphi_B$ the following result

$$\cos\frac{\varphi_B}{2} = \frac{1}{\tan\frac{\varphi}{2}}\frac{Q}{E+E'} = \sqrt{\frac{2\varepsilon}{1+\varepsilon}}. \tag{61}$$

Using Eq. (61) to substitute $\varphi_B$ in Eq. (60) in terms of $\varphi$ we will get Eq. (13).

## References


1. M.N. Rosenbluth, Phys. Rev. **79**, 615 (1950)
2. R. Hofstadter, R.W. McAllister, Phys. Rev. **98**, 217 (1955)
3. E. Chambers, R. Hofstadter, Phys. Rev. **103**, 1454 (1956)
4. P.J. Mohr, B.N. Taylor, D.B. Newell, Rev. Mod. Phys. **84**, 1527 (2012)
5. R. Pohl, R. Gilman, G.A. Miller, K. Pachucki, Annu. Rev. Nucl. Part. Sci. **63**, 175 (2013)
6. W. Xiong, A. Gasparian, Z.W. Zhao, Nature **575**, 147 (2019)
7. R. Pohl et al., Nature **466**, 216 (2010)
8. A. Antognini et al., Science **339**, 417 (2013)
9. V. Punjabi et al., Phys. Rev. C **71**, 055202 (2005)
10. A. Puckett et al., Phys. Rev. C **85**, 045203 (2012)
11. L.N. Hand, D.G. Miller, R. Wilson, Rev. Mod. Phys. **35**, 335 (1963)
12. T. Janssens, R. Hofstadter, E.B. Hughes, M.R. Yearian, Phys. Rev. **142**, 922 (1966)
13. M.E. Christy et al., Phys. Rev. C **70**, 015206 (2004)
14. I.A. Qattan et al., Phys. Rev. Lett. **94**, 142301 (2005)
15. P.G. Blunden, W. Melnitchouk, J.A. Tjon, Phys. Rev. Lett. **91**, 142304 (2003)
16. P.A.M. Guichon, M. Vanderhaeghen, Phys. Rev. Lett. **91**, 142303 (2003)
17. B.S. Henderson et al., OLYMPUS. Phys. Rev. Lett. **118**(9), 092501 (2017)
18. D.K. Hasell for the OLYMPUS Collaboration, Conf. Ser. **966**, 012053 (2018)
19. D. Borisyuk, A. Kobushkin, arXiv:1911.10956
20. A. Rafiei, Z. Rezaei, A. Mirjalili, Eur. Phys. J. C **77**, 319 (2017)
21. J. Selvaganapathy, P.K. Das, P. Konar, Phys. Rev. D **93**, 116003 (2016)
22. Z. Rezaei, S. Paktinat Mehdiabadi, J. Phys. G **46**, 105003 (2019)
23. M. Chaichian, M.M. Sheikh-Jabbari, A. Tureanu, Phys. Rev. Lett. **86**, 2716 (2001)
24. N. Kersting, Phys. Lett. B **527**(1,2), 115 (2002)
25. I. Mocioiu, M. Pospelov, R. Roiban, arXiv:hep-ph/0110011
26. X. Calmet, B. Jurco, P. Schupp, J. Wess, M. Wohlgenannt, Eur. Phys. J. C **23**, 363 (2002)
27. P. Mathews, Phys. Rev. D **63**, 075007 (2001)
28. Z. Rezaei, R. Salehi, Ann. Phys. **406**, 71 (2019)
29. Z. Rezaei, T. Alizadeh, Iran. J. Phys. Res. **19**, 455 (2019)
30. Z. Rezaei, S.P. Zakeri, arXiv:2007.01501
31. R. Horvat, D. Latas, J. Trampetić, J. You, Phys. Rev. D **101**, 095035 (2020)
32. E. Witten, Nucl. Phys. B **268**, 253 (1986)
33. N. Seiberg, E. Witten, JHEP **09**, 032 (1999)
34. J. Madore, S. Schraml, P. Schupp, J. Wess, Eur. Phys. J. C **16**, 161 (2000)
35. I.F. Riad, M.M. Sheikh-Jabbari, JHEP **0008**, 045 (2000)
36. M.R. Douglas, N.A. Nekrasov, Rev. Mod. Phys. **73**, 977 (2001)
37. C.P. Martin, D. Sanchez-Ruiz, Phys. Rev. Lett. **83**, 476 (1999)
38. R.J. Szabo, Phys. Rep. **378**, 207 (2003)

39. B. Melic, K. Passek-Kumericki, J. Trampetic, P. Schupp, M. Wohlgenannt, Eur. Phys. J. C **42**, 483 (2005)
40. B. Melic, K. Passek-Kumericki, J. Trampetic, P. Schupp, M. Wohlgenannt, Eur. Phys. J. C **42**, 499 (2005)
41. J. Gomis, T. Mehen, Nucl. Phys. B **591**, 265 (2000)
42. F.J. Ernst, R.G. Sachs, K.C. Wali, Phys. Rev. **119**, 1105 (1960)
43. W. Greiner, J. Reinhardt, *Quantum Electrodynamics*, 4th edn. (Springer, New York, 2009)
44. F. Halzen, A.D. Martin, *Quarks and Leptons: An Introductory Course in Modern Particle Physics* (Wiley, New York, 1987)
45. L. Andivahi et al., Phys. Rev. D **50**, 5491 (1994)
46. R.C. Walker et al., Phys. Rev. D **49**, 5671 (1994)
47. A.I. Akhiezer, M.P. Rekalo, Sov. Phys. Dokl. **13**, 572 (1968)
48. M.K. Jones et al., Phys. Rev. Lett. **84**, 1398 (2000)
49. O. Gayou et al., Phys. Rev. Lett. **88**, 092301 (2002)
50. A. Puckett et al., Phys. Rev. C **96**, 055203 (2017)
51. M. Meziane et al., Phys. Rev. Lett. **106**, 132501 (2011)
52. A.J.R. Puckett, arXiv:1508.01456
53. M. Haghighat, M.M. Ettefaghi, Phys. Rev. D **70**, 034017 (2004)